

SCC INITIATION FOR 4340 IN DISTILLED WATER

A ATRENS, ZF WANG* and JQ WANG*
*Department of Mining, Minerals and Materials Engineering
The University of Queensland, Brisbane Qld 4072, Australia*

**State Key Laboratory of Corrosion Science,
Institute of Corrosion and Protection of Metals,
The Chinese Academy of Sciences, Shenyang 110015, P. R. China*

ABSTRACT

SCC initiation was studied for 4340 in distilled water at room temperature. SCC initiation was consistent with the following model which couples SCC initiation with cracking of a surface protective oxide by means of a dynamic interaction between oxide formation, the applied stress, oxide cracking, pitting and the initiation of SCC. An aspect of the dynamic interaction is cracks forming in a protective surface oxide due to the applied stress, exposing to the water bare metal at the oxide crack tip, and oxidation of the bare metal causing crack healing. Oxide crack healing would be competing with the initiation of intergranular SCC if an oxide crack meets the metal surface at a grain boundary. If the intergranular SCC penetration is sufficiently fast along the metal grain boundary, then the crack yaws open preventing healing of the oxide crack. If intergranular SCC penetration is not sufficiently fast, then the oxidation process could produce sufficient oxide to fill both the stress corrosion crack and the oxide crack; in this case there would be initiation of SCC but only limited propagation of SCC. Stress induced cracks in very thin oxide can induce pits which initiate SCC, and under some conditions such stress induced cracks in a thin oxide can directly initiate SCC.

KEYWORDS

SCC Initiation, Protective Oxides, Passivity, 4340, High strength steel, ESEM

INTRODUCTION

Stress corrosion cracking (SCC) (Atrens and Wang 1995) is a complex multistep process which involves the combination of mechanical, physical and chemical processes that accomplish the separation of bonds at the initiation site or at the crack tip, thereby initiating or advancing the SCC crack. SCC often occurs under corrosive conditions where general corrosion is not a problem. The corrosion resistance of interest is caused by surface films that separate the material from its environment. Such films can cause a low rate of general corrosion despite a large thermodynamic driving force for corrosion. For example, stainless steels are stainless because of a very thin passive surface layer which is essentially Cr_2O_3 . Although, this layer is so thin (typically less than 4 nm Jin and Atrens 1987, 1990, Lim and Atrens 1992a, 1992b) that it cannot be seen with the naked eye, this layer is nevertheless effective in separating the steel from its environment. The passive films on stainless steels are usually self repairing. The breakdown of such films can be induced chemically (eg by chlorides), and pitting corrosion results when the breakdown is localised. Localised film breakdown under the joint action of a stress and an environment is the essence of SCC. Cracking of surface films has been shown to

be involved for SCC initiation in pipeline steels (Wang and Atrens 1996a, 1996b) and high strength steels (Atrens et al 1996, Oehlert and Atrens 1993, 1996).

Our prior work has dealt extensively with SCC of steels. A new test method for SCC was developed (Atrens et al 1993a, Ramamurthy and Atrens 1993): the linearly increasing stress test (LIST) and was applied to high strength steels (Atrens et al 1993a, Ramamurthy and Atrens 1993) pipeline steels (Wang and Atrens 1996a, 1996b), carbon steel (Atrens and Oehlert 1996) and pure copper (Salmond and Atrens 1992). Stress rate effects have been shown (Rieck et al 1989a) to be an important part of the SCC mechanism, and in particular crack tip creep has been shown to be important part of the SCC mechanism for high strength steels undergoing SCC in water, which can provide an explanation for the stationary cracks observed in service. Room temperature creep has been measured for high strength steels including AISI 4340 and AerMet100 (Oehlert and Atrens 1994) and related to crack initiation. A new model was proposed for SCC for quenched and tempered steels based on strain assisted dissolution (Atrens et al 1989). Stress corrosion crack velocity was related to heat treatment & microstructure (Rieck et al 1989b, 1989c). The possible causes for the intergranular crack path for high strength steels undergoing SCC in water have been explored by microstructural characterisation using electron microscopy (Gates et al 1987a, b, c), measurements of grain boundary chemistry (Skogsmo and Atrens 1994) and electrochemistry (Ramamurthy et al 1989). A precipitation strengthened duplex stainless steel was developed (Atrens et al 1993b).

Many mechanisms have been proposed for crack initiation, including: pitting (Christman 1990 and 1991), anodic dissolution (Parkins 1969 and Rhodes 1969), film rupture (McEvily and Bond 1965 and Pugh 1977) and hydrogen embrittlement (Troiano 1974 and Rhodes 1969). The development and application of micro-measurement technology is required to advance our knowledge of the processes occurring during SCC initiation. Detailed observations and measurements are needed down to the atomic level to understand the issues involved including for example the chemical influence on bond breaking. A possible step in the direction of appropriate micro-measurement technology may be provided by the environmental scanning electron microscope (ESEM) (Uwins 1994).

Specimen observation with a conventional scanning electron microscope (SEM) causes total specimen drying because of the high vacuum within the SEM. The ESEM overcomes this limitations by permitting the entire specimen chamber to be held at a much higher pressure (up to 20 torr). Simultaneously, a high vacuum is maintained in the electron gun and electron column areas by means of differential pumping of the various regions of the ESEM. Thus the ESEM can be used to observe specimens without drying them and much use has been made of the ESEM for observing physical and biological specimens in their natural state without drying (Uwins 1994). However direct observation of a specimen surface under liquid water is not possible even in the ESEM because the liquid water absorbs all of the electrons of the primary incident beam. Thus direct ESEM observation of SCC initiation requires careful experimental design; it would be possible to observe the edge of a horizontal specimen in contact with liquid water at the same level as the specimen. In developing the capability to attempt such experiments, a stressing stage has been developed for the ESEM.

This stage was used in a preliminary study to study SCC initiation for X52 steel in a carbonate-bicarbonate solution (Atrens et al 1996, Wang and Atrens 1996b). This indicated that SCC initiation involved the formation and cracking of a surface oxide film. Moreover, this work highlighted the limitation of the ESEM in such research in that SCC of pipeline steels in carbonate-bicarbonate solutions is a relatively slow process, even though this is a typical SCC system. This limitation might be overcome by the study of a model system where the SCC processes are much faster such as 4340 high strength steel in water in which case there are high SCC velocities in the range 1×10^{-4} to 1×10^{-7} m/s and that is the purpose of the work reported in this paper. This paper presents ESEM observations of SCC initiation for 4340 high strength steel in distilled water. Possible SCC initiation mechanisms are proposed. In this study the use of the ESEM has the advantage over a SEM in that the specimen surface is not dried during the ESEM observation.

EXPERIMENTAL PROCEDURE

The material was 4340 high strength steel with chemical composition as shown in Table 1. A flat tapered specimen shape was used. To prevent distortion, all specimens were held by a jig during heat treatment: austenitized 2 hr at 860°C in high-purity argon and oil quenched. The yield strength was 1270 MPa. After heat treatment, the specimen gauge sections were polished with 800 grit emery paper.

Table 1 Chemical Composition (wt%)

C	Cr	Ni	Mn	Mo	P	S	Si	V
0.36	1.64	1.50	0.6	0.25	0.01	0.005	0.30	0.06

The loading stage has been described previously; this could be installed and moved freely in the ESEM chamber. This loading stage and choice of tapered specimen shape allowed a constant load to be applied to each specimen with the result that there was a range of stress values along the specimen; the stress values decreased with distance along the specimen from the maximum stress at the minimum section. In the SCC experiments reported in this paper, each specimen was subjected to a tension stress of 1450 to 1500 MPa at the narrowest part. Prior to testing, each specimen was cleaned using alcohol and distilled water, and the specimen was immediately mounted into the loading stage. The distilled water was poured into the cell to cover the specimen surface and simultaneously the tensile stress was applied. All experiments were carried out in aerated distilled water at room temperature at the free corrosion potential. During the SCC experiments, the specimen surface was covered by the water. Unfortunately, ESEM observations of the specimen surface are not possible through a water layer, (because the electrons of the primary beam would be all absorbed in such a layer). To enable ESEM observation of the specimen surface, the water level was lowered below the specimen, causing an interruption of the SCC exposure. Such observations were carried out using 6 separate specimens after total exposure times of 1, 4, 12, 15, 24 and 48 h.

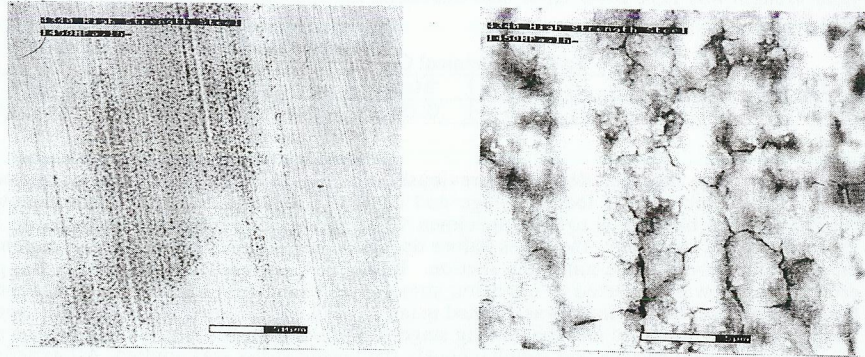
RESULTS

Fig. 1 shows the specimen surface appearance for specimen A after 1 hr of exposure at stress to distilled water. It could be seen with the naked eye that rust (brown in colour) covered some parts of the surface. After the rust was removed by light brushing, an oxide film (dark in colour) could be seen on the specimen surface; this is illustrated in Fig. 1(a) where the parts appearing like a shadow correspond to this dark oxide film. When this area was examined at greater magnification, it became clear that some areas were continuously covered with an oxide of significant thickness which had many fine cracks as shown in Fig. 1(b). These small cracks did not seem to be related to metal grain boundaries because the distribution of these cracks was smaller than the grain size. There were also pits on the oxide film, but no SCC initiation was caused by these pits.

ESEM observations of specimen A were carried out for a second time after a further 3 hr exposure to distilled water under stress which corresponds to a total exposure time of 4 hr. Again brown rust covered part of the surface. This was very loose and was easily removed by brushing. After the brown rust was removed, the dark oxide film with cracks was visible, Fig. 2.

Specimen B (4340 continuously exposed for 12 hr to distilled water at stress) gave a similar result. The size and morphology of these oxide cracks was very similar to the grain size as observed on a typical SCC fracture surface as shown in Fig. 3 for specimen D. The SCC fracture surface showed totally intergranular SCC cracking as expected for SCC of high strength steels in water. This provided a strong indication that the oxide cracks shown in Fig 2 were probably initiating SCC and furthermore, the oxide film that caused the SCC initiation was thick compared to the oxide film covering other areas of the surface. Note that the oxide crack morphology shown in Fig. 2 typical after exposure for 4 h and 12 h to distilled water under stress is significantly different to the oxide crack morphology as illustrated in Fig. 1(b) typical for 1 hr exposure to distilled water under stress. This leads to the issue of how the oxide cracks

observed after 1 hr exposure to water under stress could transform to give a crack morphology similar to that of the grain boundaries as observed for the oxide cracks after longer exposure to distilled water under stress.



(a)

(b)

Fig. 1 Surface appearance after 1 h exposure to distilled water under load. (a) overview. (b) higher magnification view showing cracks in thick oxide.

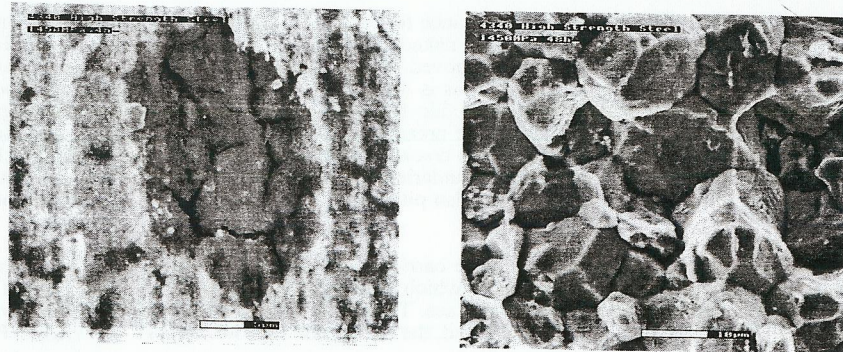


Fig. 2 Oxide film after 4h exposure of specimen to distilled water under load. Note cracks with a morphology and distribution corresponding to metal grain boundaries.

Fig. 3 Intergranular SCC.

ESEM observations of specimen *A* were carried out for a third time after a further 11 hours

exposure to distilled water under stress which corresponds to a total exposure time of 15 hours. All the specimen surface was covered by an oxide film at this time although the oxide thickness varied from place to place. In areas where there was thick oxide, the cracks in the oxide were large, and the crack shape and size was related to the grain size and morphology as illustrated previously in Fig. 2. These cracks had become large and connected with each other perpendicular to the loading direction. It is thought that there were many small cracks and that some of these had linked together perpendicular to the direction of the maximum tensile stress and thereby had become quite long in this direction. Fig. 4 illustrates that in areas of thin oxide it was common for a line of pits to initiate in a line perpendicular to the tensile direction, and for these pits to initiate SCC which linked the pits. Fig 4 shows a case where SCC has joined at least 4 distinct pits. There was also SCC initiation at the edge of the specimen. Both the pits and the specimen edge are sites with a high stress concentration where SCC was observed to initiate easily.

Specimen *D* after continuous exposure of 24 h to water at stress indicated easy SCC initiation at the edge and the middle part of the specimen. In the middle part of the specimen, the SCC cracks were initiated at the bottom of the pits and then connected each other. Many pits formed at this time. Unlike pipeline steel in carbonate-bicarbonate solution, most pits caused SCC initiation. Specimen *D* after a total exposure time of 48 hr in water, indicated nearly the same results as with 24 hr exposure. The SCC cracks had become larger and connected.

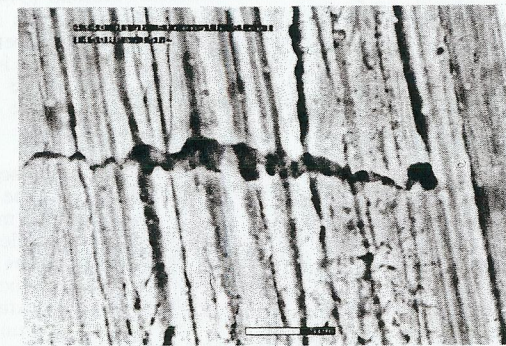


Fig. 4 In areas of thin oxide for specimen *A* after a total exposure of 15 hours to distilled water at stress it was common for a line of pits to initiate with the line perpendicular to the tensile direction, and for these pits to initiate SCC which linked the pits.

Specimen *E* was exposed to water with no applied stress to observe the oxide film formation characteristics. Oxide film formation with no applied stress was more difficult than under conditions of applied stress. There was no observable change on the specimen surface for up to 6 hr of exposure to water. After 24 hr of exposure to water a few parts of the specimen surface were covered with an oxide film. At some sites, the oxide film was thick and at the other sites, the oxide film was thin, whilst on the most parts of the specimen, there was no visible oxide film. There were cracks in the thick oxide film which were similar to those shown in Fig. 1(b).

DISCUSSION

The oxide film started to form on the specimen surface soon after the specimen was exposed to water at an applied stress. At the beginning, the oxide film occurred at a few sites. More oxide grew on the specimen surface with increasing time until it covered all the specimen surface. In places where the oxide was thick, the oxide film was obviously in two layers, with brown rust on top of a blacker oxide. The rust layer was very easily removed by brushing, and thus was very lightly bound to the substrate. It is expected that this brown rust had no influence on SCC initiation which was associated with the more adherent oxide which was black in colour when it was of sufficient thickness.

The oxide film became thicker with increasing time. However, the thickness of the oxide film was different at different sites. It was thick at some places and thin at other places. Unlike the oxide film for pipeline steel in carbonate-bicarbonate solution, which was mainly associated with the applied potential and less with applied stress, the oxide film for 4340 high strength steel in water at the free corrosion potential was mostly associated with applied stress as is clear from a comparison of experiments exposing the 4340 specimens to distilled water with and without load.

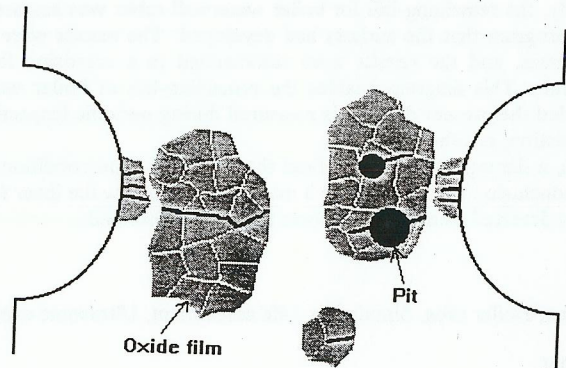


Fig. 5 The three circumstances observed to cause the initiation of SCC.

The oxide film is a necessary part of the process in the initiation of SCC cracks. Fig. 5 summarises the observations for 4340 high strength steel in distilled water. Three initiation circumstances were observed: (1) thick oxide film cracking leading to SCC in the metal, (2) the initiation of pits initiating SCC in the metal and (3) SCC initiating from the edge of the specimen. For the first case, the cracks in the thick oxide film easily initiated SCC cracks due to the high stress concentration and appropriate chemistry inside the cracks. The fracture surface appearance shown in Fig. 3 indicated an intergranular path for SCC propagation. Fig 2 also show that SCC initiated intergranularly. These observations indicated that only the large oxide cracks with an appropriate orientation, for example, perpendicular to the applied stress direction, are favoured to initiate SCC cracks.

Note that the oxide crack morphology shown in Fig. 2 typical after exposure for 4 hr and 12 hr to distilled water under stress respectively was significantly different to the oxide crack

morphology as illustrated in Fig. 1(b) typical for 1 hr exposure to distilled water under stress. This leads to the issue of how the oxide cracks observed after 1 hr exposure to water under stress could transform to give a crack morphology similar to that of the grain boundaries as observed for the oxide cracks after longer exposure to distilled water under stress as typified by Fig. 2.

Oxide cracks were observed experimentally to form preferentially at metal grain boundaries for specimens exposed to the water for times longer than one hour. Such oxide cracks could be imagined to concentrate appropriate conditions onto the metal surface to easily initiate SCC in the underlying metal at the grain boundaries. It is also possible that such cracks would preferentially initiate grain boundary SCC in the metal only when there was a coincidence between an oxide crack and a metal grain boundary. If such a crack was not appropriately located to initiate SCC in an underlying grain boundary, then it would be expected for such an oxide crack to heal as part of the continuing oxidation of the metal surface, as oxide formation would be expected to be particularly fast at an existing oxide crack due to the easy access of the solution to bare metal. Thus oxide cracks could be in a continuous state of formation and repair with only those corresponding to metal grain boundaries remaining after significant exposure times when SCC had initiated in the grain boundaries below the oxide cracks. In this view there is a direct interaction of SCC initiation in the metal which would cause a yawing open of the oxide crack and thereby prevent sufficient oxidation of the metal (which would cause the crack to heal). This provides a dynamic model of oxide cracks forming due to the applied stress, exposing the water bare metal at the oxide crack tip, and oxidation of the bare metal causing crack healing. Oxide crack healing would be competing with the initiation of intergranular SCC if the oxide cracks meet the metal surface at a grain boundary. If intergranular SCC penetration is sufficiently fast along the metal grain boundaries, then the crack yaws open preventing healing of the oxide crack. If intergranular SCC penetration is not sufficiently fast, then the oxidation process could produce sufficient oxide to fill both the stress corrosion crack and the oxide crack; in this case there would be initiation of SCC but only limited propagation of SCC. Such SCC initiation and limited propagation is a common observation in pipeline steels and could correlate in the above mechanism with a slow crack propagation velocity.

This mechanism has considerable support from the observations that stress accelerates the oxide film formation. A strong possibility for the mechanism by which stress could accelerate oxide film formation is a mechanism of oxide cracking exposing bare metal to corrosion/oxidation by the distilled water. Further strong support for an applied stress causing oxide film cracking comes from the observation of stress induced pitting and the linking of such pits by stress corrosion cracks oriented perpendicular to the direction of maximum tensile stress as shown in Fig. 4. There does not seem to be any other reason why pits should become oriented with respect to the tensile stress; these results argue that the tensile stress has a major role in pit initiation by local oxide cracking.

Similarly, in this emerging model, stress would be involved in the initiation of SCC at the specimen edge because the edge is a stress concentrator. The mechanism would be oxide cracking caused by the stress concentration at the specimen edge. This mechanism is proposed on the basis that there would be a thin oxide covering all the specimen surface even in places where this oxide is not sufficiently thick to be obvious.

CONCLUSIONS

An applied stress was found to accelerate the formation of oxide film on the specimen. Many small cracks were observed on the thick oxide film. Pits were formed on the thin oxide film. SCC was observed to initiate in the following circumstances: (1) thick oxide film cracking leading to intergranular SCC in the metal, (2) the initiation of pits initiating SCC in the metal and (3) SCC initiating from the edge of the specimen.

All these three initiation circumstances are consistent with the following model which couples SCC initiation with cracking of a surface protective oxide. There is oxide formation on the metal surface. There is a dynamic interaction between oxide formation, the applied stress, oxide

cracking, pitting and the initiation of SCC. An aspect of the dynamic interaction is cracks forming in a protective surface oxide due to the applied stress, exposing to the water bare metal at the oxide crack tip, and oxidation of the bare metal causing crack healing. Oxide crack healing would be competing with the initiation of intergranular SCC if the oxide cracks meet the metal surface at a grain boundary. If intergranular SCC penetration is sufficiently fast along the metal grain boundaries, then the crack yaws open preventing healing of the oxide crack. If intergranular SCC penetration is not sufficiently fast, then the oxidation process could produce sufficient oxide to fill both the stress corrosion crack and the oxide crack; in this case there would be initiation of SCC but only limited propagation of SCC. Stress induced cracks in very thin oxide can induce pits which initiate SCC, and under some conditions such stress induced cracks in thin oxide can directly initiate SCC.

ACKNOWLEDGMENT

This work was supported by East Australia Pipeline Ltd.

REFERENCES

- Atrens, A, RM Rieck and IO Smith (1989). *ICF7 Advances in Fracture Research*, K Salama, K Ravi-Chandar, DMR Taplin, P Rama Rao eds, Pergamon Press, pp 1603.
- Atrens, A, CC Brosnan, S Ramamurthy, A Oehlert and IO Smith (1993a). *Measurement Science and Technology*, **4**, 1281.
- Atrens, A, R Coade, J Allison, H Kohl, G Hochoertler and G Krist (1993b). *Materials Forum*, **17**, 263.
- Atrens, A and ZF Wang (1995). *Materials Forum*, **19**, 9.
- Atrens, A and A Oehlert (1996). *J Materials Science*, submitted for publication.
- Atrens, A, ZF Wang, N Kinaev, DR Cousens and JQ Wang (1996). *13 ICC*, Melbourne.
- Christman, TK (1990) *Corrosion*, **46** 450.
- Christman, TK (1991) *Materials Performance*, **30**, 23.
- Gates, JD, A Atrens, and IO Smith (1987a). *Z fur Werkstofftechnik*. **18**, 165
- Gates, JD, A Atrens, and IO Smith (1987b). *Z fur Werkstofftechnik*. **18**, 179.
- Gates, JD, A Atrens, and IO Smith (1987c). *Z fur Werkstofftechnik*. **18**, 344.
- Jin, S and A Atrens (1987). *Applied Physics A*, **42**, 149.
- Jin, S and A Atrens (1990). *Applied Physics A*, **50**, 287.
- Lim, AS and A Atrens (1992a). *Applied Physics A*, **53**, 273.
- Lim, AS and A Atrens (1992b). *Applied Physics A*, **54**, 500.
- Mcevely, AJ and A. P. Bond, (1965) *J. Electrochem. Soc.*, **112** 112.
- Oehlert, A and A Atrens (1993). *Materials Forum*, **17**, 415-429.
- Oehlert, A and A Atrens (1994). *Acta Metallurgica et Materialia*, **42**, 1493-1508.
- Oehlert, A and A Atrens (1996). *Corrosion Science* **38**, 1159.
- Parkins, RN (1969) *Fundamental Aspects of SCC*; ed. by R. W. Staehle, A. J. Forty and D. V. Rooyen, Houston, TX., NACE, 361.
- Pugh, EN (1977) *The Theory of SCC in Alloys*, ed. by J. C. Scully, NATO, Brussel, 21.
- Ramamurthy, S A Atrens, IO Smith (1989). *Materials Science Forum* **44 & 45**, 139.
- Ramamurthy, S and A Atrens (1993). *Corrosion Science*, **34**, 1385.
- Rhodes, PR (1969) *Corrosion*, **25** 462.
- Rhodes, PR (1969) *Corrosion*, **25** 462.
- Rieck, RM, A Atrens and IO Smith (1989a). *Met Trans*, **20A** 889.
- Rieck, RM, A Atrens and IO Smith (1989b). *Materials Forum*. **13**, 48.
- Rieck, RM, A Atrens and IO Smith (1989c). *Materials Forum*. **13**, 54.
- Salmond, J and A Atrens (1992). *Scripta Metallurgica et Materialia*. **26**, 1447-1450.
- Skogsmo, J, and A Atrens (1994). *Acta Metallurgica et Materialia* **42**, 1139.
- Troiano, AR (1974) *Hydrogen in Metals*, ed. by I. M. Bernstein, 12.
- Uwins, PJR (1994). *Materials Forum* **18**, 51.
- Wang, ZF and A Atrens (1996a). Accepted for publication in *Metall and Mat Trans A*.
- Wang, ZF and A Atrens (1996b). submitted for publication in *Acta Materialia*.